

## Assessing the quality of Aeolus wind over a tropical location (10.04 N, 76.9 E) using 205 MHz wind profiler radar

Ajil Kottayil, K Prajwal, M V Devika, S Abhilash, K Satheesan, Roshny Antony, Viju O. John & K Mohanakumar

To cite this article: Ajil Kottayil, K Prajwal, M V Devika, S Abhilash, K Satheesan, Roshny Antony, Viju O. John & K Mohanakumar (2022) Assessing the quality of Aeolus wind over a tropical location (10.04 N, 76.9 E) using 205 MHz wind profiler radar, International Journal of Remote Sensing, 43:9, 3320-3335, DOI: [10.1080/01431161.2022.2090871](https://doi.org/10.1080/01431161.2022.2090871)

To link to this article: <https://doi.org/10.1080/01431161.2022.2090871>



Published online: 27 Jun 2022.



Submit your article to this journal [↗](#)



View related articles [↗](#)



View Crossmark data [↗](#)



## Assessing the quality of Aeolus wind over a tropical location (10.04 N, 76.9 E) using 205 MHz wind profiler radar

Ajil Kottayil<sup>a</sup>, K Prajwal<sup>a</sup>, M V Devika<sup>a</sup>, S Abhilash <sup>a,b</sup>, K Satheesan<sup>a,b</sup>, Roshny Antony<sup>a,b</sup>, Viju O. John<sup>c</sup> and K Mohanakumar<sup>a</sup>

<sup>a</sup>Advanced centre for Atmospheric Radar Research, Cochin University of Science and Technology, Cochin, India; <sup>b</sup>Department of Atmospheric Sciences, Cochin University of Science and Technology, Cochin, India; <sup>c</sup>EUMETSAT, Eumetsat Allee 1, 64295 Darmstadt, Germany

### ABSTRACT

Aeolus is European Space Agency's unique and novel wind measuring satellite mission providing near real-time wind profiles from near surface to an altitude of 30 km. This paper presents the validation of Aeolus wind profiles over Cochin (10.04° N, 76.9°E), India using the 205 MHz wind profile radar. The Aeolus wind profiles (baselines 10 and 11) have been validated for an altitude range of 1 to 18 km during June, 2019 to September, 2021. Aeolus Rayleigh wind for clear (Rayleigh<sub>clear</sub>) and Mie wind for cloudy (Mie<sub>cloudy</sub>) show very good agreement with the radar wind profiles. The Pearson correlation coefficient between radar and Aeolus wind for Rayleigh<sub>clear</sub> and Mie<sub>cloudy</sub> are 0.93 and 0.94, respectively. The systematic and random errors in Rayleigh<sub>clear</sub> are found to be  $-0.15 \text{ m s}^{-1}$  and  $4.87 \text{ m s}^{-1}$ , respectively, while these values are  $-0.06 \text{ m s}^{-1}$  and  $3.68 \text{ m s}^{-1}$  for Mie<sub>cloudy</sub>. A detailed error characterization of Aeolus wind profiles with respect to radar is presented in this study. The bias in Aeolus wind is provided in terms of observation altitude, seasons, different windy conditions and ascending/descending orbits.

### ARTICLE HISTORY

Received 11 February 2022  
Accepted 10 June 2022

### KEYWORDS

Aeolus; 205 MHz radar; tropics; validation

## 1. Introduction

Wind is a vital climate variable, primarily responsible for the dynamic nature of the atmosphere. It is both a cause as well as effect in meteorology. Winds vary depending on their scales, direction of flow, speeds and latitudes. General circulation refers to the distribution of winds over the Earth and governs the weather and climate and is thus an essential element for forecasts of weather. Conventionally, wind speed and direction have been measured using instruments like anemometers, wind vanes, radiosondes, lidar, wind profilers etc. These instruments yield point measurements for regional scale studies. Wind measurements are crucial in several areas ranging from agriculture to wind energy harvesting. In meteorology, wind has huge relevance for studies on turbulence, waves, energy and momentum transport, large-scale transportation of pollution and trace gases

**CONTACT** Ajil Kottayil  [ajil.acarr@cusat.ac.in](mailto:ajil.acarr@cusat.ac.in)  Advanced centre for Atmospheric Radar Research, Satellite Remote Sensing and Applications Advanced Centre for Atmospheric Radar Research, Cochin University of Science and Technology, Cochin, India

among several others (Satheesan and Krishna Murthy 2002; Kottayil et al. 2018; Legras and Bucci 2020). Again, wind measurements are sparse or almost non-existent over vast oceanic regions and remote polar locations.

Wind measurements are crucial in some regions like the tropics. In mid-latitudes, there is a direct relationship between pressure fields and wind. Therefore, it is easier to infer wind direction and speed by simply referring to isobars or surface charts. But the pressure gradients in the tropics are quite weak and inferring wind from pressure gradients is not a feasible method. Alternatively, cloud motion wind can be derived from Geo-stationary satellite imagery but they are often affected by uncertainties with cloud top height assignments (Nieman, Schmetz and Paul Menzel 1993; Schmetz et al. 1993). Also, detailed profiles of wind cannot be obtained from this method.

To ameliorate the issues pertaining to wind measurements to a large extent, the European Space Agency (ESA) came up with Aeolus, a novel scientific mission that provides vertically resolved global wind profiles from space using an active Doppler wind Lidar technique (Reitebuch 2012). Near real-time measurements of wind profiles can be obtained from the surface up to an altitude of 30 km. One of the main objectives of the mission is to improve the numerical weather prediction models through the assimilation of global wind profiles. The usefulness of this data in improving weather forecasts, particularly over the tropics has been demonstrated by preliminary studies (Rennie and Isaksen 2020; Rennie et al. 2021). These data are major asset to the global observing system that can improve understandings of Earth's energy budget, exchange processes, global circulation and associated weather phenomena. Since, Aeolus is the first of its kind wind data, there is a need to understand and characterize the errors in its profiles. This can help in optimizing the data by correcting for errors and biases and thus enhance the performance of weather prediction.

Several studies have dealt with the validation of Aeolus wind in other regions of the world. Radiosondes have been used to assess the systematic and random errors in Aeolus 2B02 wind over the Atlantic Ocean (Baars et al. 2020). Martin et al. (2021) compared Aeolus wind against radiosondes and numerical weather prediction model wind fields over the northern hemisphere. Iwai et al. (2021) evaluated the quality of Aeolus wind baselines 2B02 and 2B11 over Japan using wind profiler radar, lidar and radiosondes. Quality assessment of Aeolus wind over Antarctica and northern Sweden is given in Belova et al. (2021). Validation of Aeolus wind using wind profiler radar, ground-based Rayleigh–Mie Doppler lidar and airborne campaign Doppler lidar data is given elsewhere (Lux et al. 2020; Khaykin et al. 2020; Witschas, Lemmerz, and Reitebuch 2012).

The present study has been fulfilled as a part of assessing the quality of Aeolus wind profiles over Cochin (10.04° N, 76.9°E), a tropical location, using data from 205 MHz wind profiler as reference for the first time. A comprehensive validation of Aeolus wind over a tropical location using this dedicated wind profiler radar facility will also help in understanding the amount of agreement/disagreement in systematic and random errors in Aeolus wind over the tropics in comparison to other regions of the world. The wind profiler radar is operational since 2017 and provides three-dimensional wind profiles for an altitude range of 315 m to 20 km. The radar's location is in a key region with diverse weather patterns and is a hotbed for circulations of varying strengths. Using more than two years of radar data, a detailed error characterization of Aeolus wind profiles is provided in this study.

## 2. Data and methodology

### 2.1. 205 MHz wind profiler radar

The 205 MHz wind profiler radar is an active-phased array radar, having 619 antenna elements capable of probing the atmosphere from 315 m to 20 km. The effective aperture area and power aperture product of the radar are 536 m<sup>2</sup> and 1.6x10<sup>8</sup> Wm<sup>2</sup>, respectively (Mohanakumar et al. 2017). Three-dimensional wind profiles can be generated from this radar at high temporal and spatial resolutions. Depending on the height, the field of view of the radar may vary from 175 m at 500 m to 7 km at 20 km. The radar provides precise measurements of wind, and the bias in its horizontal wind component with respect to radiosonde is below 0.5 m s<sup>-1</sup> within 315 m to 18 km; however, the random error ranges from 1.5 m s<sup>-1</sup> within 500 m-12 km to 2.7 m s<sup>-1</sup> within 12–18 km (Kottayil et al. 2016; Mohanakumar et al. 2017).

The radar is generally operated at three different coded modes yielding profiles at vertical resolutions of 45 m, 180 m and 360 m. In the present study, the horizontal wind profiles from the radar between 1 and 18 km for July 2019 to September 2021 have been used for Aeolus validation. The radar data from 1 to 3 km used in this study has 45 m vertical resolution and the data within 3–18 km has 180 m resolution. The radar retrieves three-dimensional wind using Doppler beam swinging (DBS) method. In this method, radar pulses are sent in zenith and off zenith directions, the azimuth angle of which are orthogonal to one another. The signal received by the radar from different beams are Doppler shifted relative to the transmitted beams due to atmospheric motion. The Doppler shift is then used to determine the mean radial velocities of the scatterers within the field of view of the radar and thereby the three-dimensional wind velocities at different altitudes are inferred. The radar has proven to be useful in various atmospheric studies (Kottayil et al. 2018; Nithya, Kottayil and Mohanakumar 2019; Kottayil et al. 2020; Sujithlal et al. 2022). The parameters used for radar operation are given in Table 1.

### 2.2. Aeolus

The European Space Agency's Earth Explorer mission launched Aeolus satellite on 22 August 2018. Aeolus is a polar orbiting satellite, revolving at an altitude of 320 km. It carries a Doppler wind lidar called ALADIN (Atmospheric LAsER Doppler INstrument)

**Table 1.** Radar configuration.

Parameters	Specification
Frequency	205 MHz
Bandwidth	5 MHz
Half power beam width	3.2°
Height Resolution	45 m, 180 m
Peak Power Aperture product	1.6x10 <sup>8</sup> Wm <sup>2</sup>
Off-Zenith Angle	10°
Azimuth Angle	0°, 90°, 180° & 270°
Baud	0.3μs, 1.2 μs
Code length	16 bit
Pulse Repetition Frequency	5000 Hz
No. of coherent integration	256
Duty Ratio	9.76%

which is the first of its kind in the orbit. ALADIN provides profiles of the line-of-sight (LOS) wind perpendicular to satellite velocity from surface to 30 km altitude range. ALADIN emits laser pulses in the ultraviolet spectral region (354.8 nm). The backscattered signal which is Doppler shifted is collected by a dual channel receiver to measure signatures of both molecular (Rayleigh channel) and particular (Mie channel) scattering (Stoffelen et al. 2005; Reitebuch 2012; ECMWF:Rennie et al. 2020). This study uses Aeolus L2B product, Horizontal LOS (HLOS) observations for baselines 10 (2B10) and 11 (2B11) over the period, July 2019 to September 2021.

### 2.3. Methodology

The radar and Aeolus wind datasets are collocated spatially, temporally and vertically prior to their comparison. As a first step, a search radius of 100 km around the radar location was defined and the data from Aeolus overpasses within this search radius are retained. In the second step, the wind profiles which fall within  $\pm 2$  hours around the Aeolus overpass times are averaged. In the third step, the HLOS wind from the Aeolus is matched with radar zonal and meridional wind components where their altitude difference is less than 25 m. The data from radar which is 3 range bins above and below the closest altitude of Aeolus are averaged. This is because the vertical resolution of Aeolus wind varies from 250 m to 2 km depending on the altitude. Once the collocated datasets are obtained by the above processes, for facilitating a direct comparison between Aeolus and radar wind, the HLOS radar wind is calculated using the following equation.

$$\text{HLOS}_{\text{Radar}} = -U_{\text{Radar}} \sin(\phi_{\text{Aeolus}}) - V_{\text{Radar}} \cos(\phi_{\text{Aeolus}}) \quad (1)$$

where  $U_{\text{Radar}}$  and  $V_{\text{Radar}}$  are zonal and meridional wind components from the radar and  $\phi_{\text{Aeolus}}$  is the azimuth from the laser scattering volume to the satellite (Belova et al. 2021).

Certain quality flagging measures were applied on both Aeolus and radar wind before their one-to-one comparison. Those Aeolus wind measurements (both Rayleigh and Mie) where the error estimate is greater than  $6 \text{ m s}^{-1}$  and the quality flag is zero, are eliminated. The wind components from radar are also excluded based on the vertical velocity, retaining only those measurements where the absolute value of vertical velocity is less than  $0.5 \text{ m s}^{-1}$ . Generally, the magnitude of vertical velocity lies below  $1 \text{ m s}^{-1}$  but certain conditions like rain or passage of flight above the radar scanning volume may cause the vertical velocity to show anomalies. In such cases, the retrieval of horizontal wind from the radar may not be accurate. This is a caveat in data processing and not related to the radar system's performance. The radar location is shown in Figure 1.

### 3. Results

In this section, we present the results of comparisons between the radar and Aeolus HLOS wind, as a function of altitude, seasons, wind speed ranges and Aeolus ascending/descending orbits. To quantify the difference between radar and Aeolus wind, various statistical metrics such as bias, standard deviation (SD) and median absolute deviation are used. Bias represents the systematic error in the comparison, whereas SD gives the random error. However, the standard deviation overestimates the random error when there are outliers in the data. In order to reduce the weights of outliers, a modified

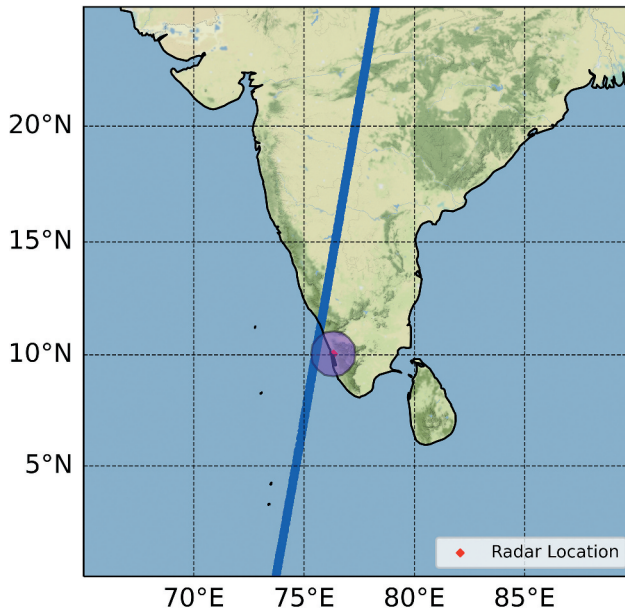


**Figure 1.** Map showing the radar location and Aeolus overpass (blue colour). The radius of the circle is 100 km which is the search radius for collocations.

relationship is proposed which is called the scaled median absolute deviation (SMAD) and is given in (2). This will provide a better measure of random error in Aeolus wind (Lux et al. 2020).

$$\text{SMAD} = 1.48 \times \text{median}(|V_{\text{diff}} - \text{median}(V_{\text{diff}})|) \quad (2)$$

where  $V_{\text{diff}}$  is the difference between Aeolus and radar HLOS wind.

### 3.1. Overall comparison between radar and Aeolus

As mentioned earlier, we have used a threshold of  $6 \text{ m s}^{-1}$  on wind error estimate to exclude Aeolus data from validation. The justification for doing so is given in Figure 2. In both Rayleigh scattering for clear sky conditions ( $\text{Rayleigh}_{\text{clear}}$ ) and Mie scattering for cloudy conditions ( $\text{Mie}_{\text{cloudy}}$ ), the difference in Aeolus wind from radar grows larger beyond  $6 \text{ m s}^{-1}$  and below this value, the differences are comparatively lower and steady. Studies have used different values for wind error estimate threshold, for example Witschas et al. (2020) have used a threshold of  $8 \text{ m s}^{-1}$  for  $\text{Rayleigh}_{\text{clear}}$  and  $4 \text{ m s}^{-1}$  for  $\text{Mie}_{\text{cloudy}}$ . This is based on how the errors grow as a function of wind error estimate in their comparison. We have also tried with these thresholds and concluded that the overall interpretation of statistics do not change significantly than shown in Table 2.

A one-to-one comparison between radar and Aeolus HLOS wind for an altitude range of 1–18 km for  $\text{Rayleigh}_{\text{clear}}$  and  $\text{Mie}_{\text{cloudy}}$  is shown in Figure 3(a,b). The Aeolus wind shows very good agreement with radar with a Pearson correlation coefficient (R) of 0.93 for  $\text{Rayleigh}_{\text{clear}}$  and 0.94 for  $\text{Mie}_{\text{cloudy}}$ . The linear regression slopes are quite close to unity and

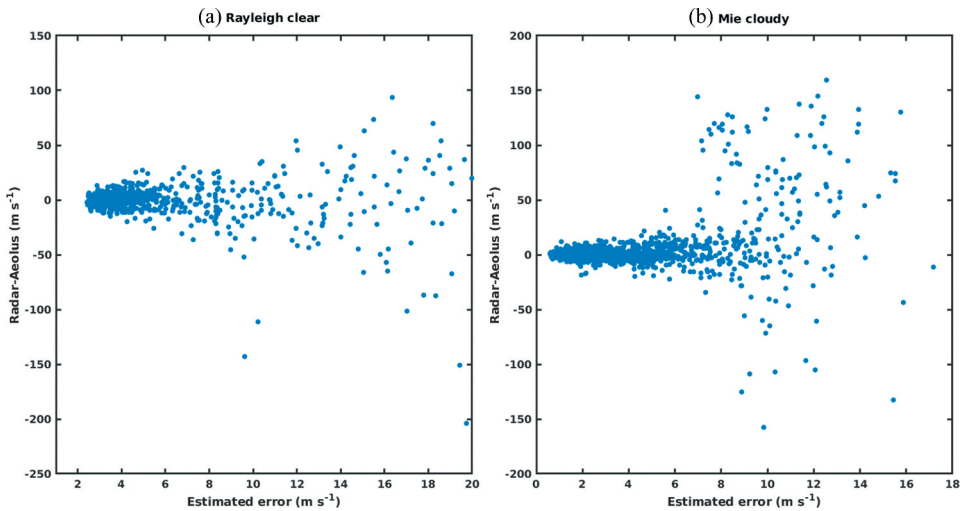


**Figure 2.** Differences between radar and Aeolus HLOS wind speed as a function of HLOS error estimate given in 2B11 for (a) Rayleigh clear and (b) Mie cloudy.

these values are 1.017 and 0.99, respectively, for Rayleigh<sub>clear</sub> and Mie<sub>cloudy</sub> winds. The bias, standard deviation and SMAD observed in Rayleigh<sub>clear</sub> are  $-0.15 \text{ m s}^{-1}$ ,  $5.49 \text{ m s}^{-1}$  and  $4.87 \text{ m s}^{-1}$ , whereas these values are lower for Mie<sub>cloudy</sub> and are  $-0.06 \text{ m s}^{-1}$ ,  $4.80 \text{ m s}^{-1}$  and  $3.68 \text{ m s}^{-1}$ , respectively.

The histogram of the differences between Aeolus and radar wind is shown in Figure 3 (c,d). It is evident that the differences lie within  $\pm 5 \text{ m s}^{-1}$  for more than 90% of the collocated data in both Rayleigh<sub>clear</sub> and Mie<sub>cloudy</sub>. Differences larger than  $15 \text{ m s}^{-1}$  are also observed, but the number of data points that accounted for these differences are very small and is less than 3% of the total collocated pairs.

Statistics have been worked out for the ascending and descending orbits for Rayleigh<sub>clear</sub> and Mie<sub>cloudy</sub> and the results are summarized in Table 2. It can be seen that systematic and random errors do not differ much between the ascending and descending orbits and these values are close to that observed for pooled datasets for both Rayleigh and Mie winds. The Rayleigh<sub>clear</sub> and Mie<sub>cloudy</sub> ascending orbits show a bias of  $-0.06 \text{ m s}^{-1}$  and  $-0.075 \text{ m s}^{-1}$ , respectively while the corresponding values for SMAD are  $4.7 \text{ m s}^{-1}$  and  $3.67 \text{ m s}^{-1}$ . However, these values are higher for descending orbit and can partially be attributed to the fewer data points as compared to the ascending orbits (see Table 2). This is because the days when radar is operated in early morning hours (coincides with descending orbits) are less as compared to evening hours. Overall, the comparison results show that the systematic and random errors are lower in Mie<sub>cloudy</sub> wind as compared to Rayleigh<sub>clear</sub>. We have also made comparisons between Aeolus and radar wind by restricting the temporal differences between them to  $\pm 1$  hours and the results are summarized in Table 2. This will yield close values for systematic and random errors as observed for a temporal difference of  $\pm 2$  hours.

The quality of the 2B10 wind product with temporal differences of  $\pm 1$  and 2 hours between collocated pairs is also evaluated separately and the results are summarized in Table 3. Note that the 2B10 product was available only during July 2019 to

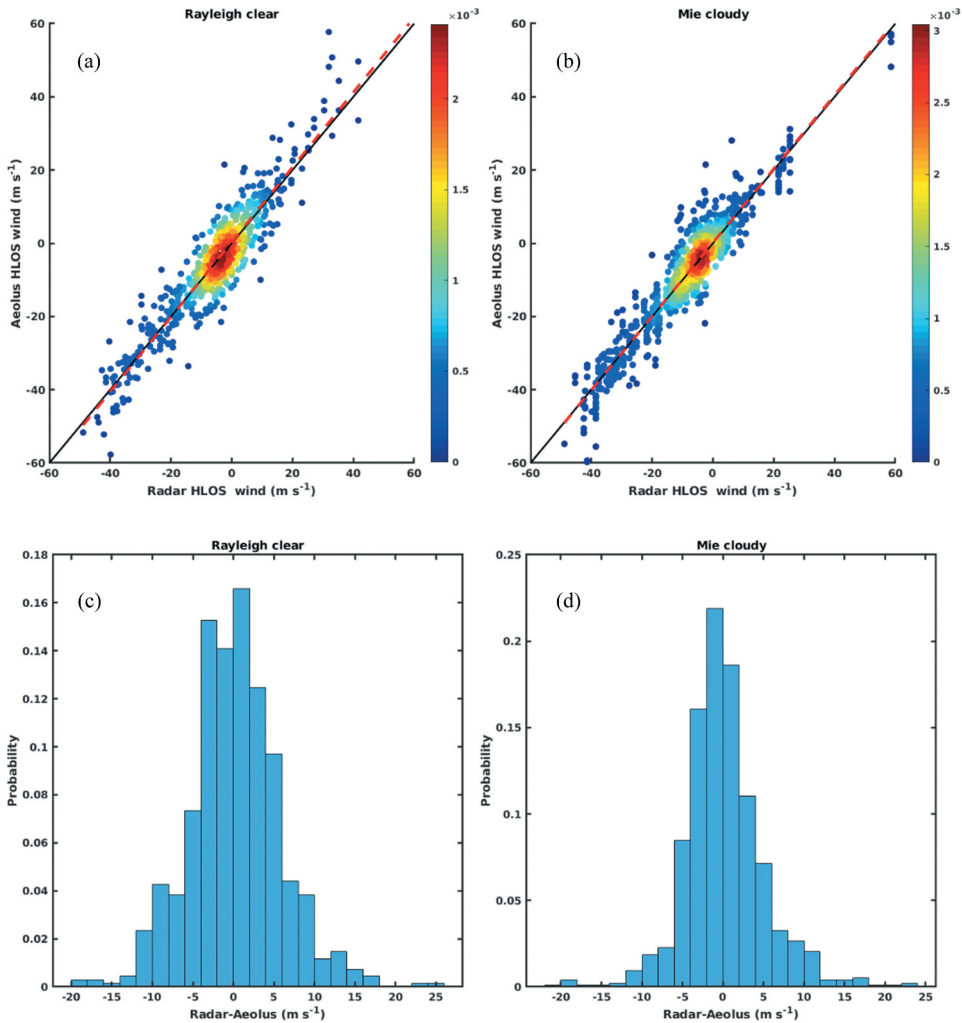


**Figure 3.** Scatter plot between radar and Aeolus wind for (a) Rayleigh clear and (b) Mie cloudy for 2B11. The black line is the diagonal line and the dotted red line is linear regression line. Colour bar shows probability density. The histogram of the difference between Aeolus and radar HLOS wind (c) Rayleigh<sub>clear</sub> and (d) Mie<sub>cloudy</sub>. Data time period is from July 2019 to September 2021.

September 2020 in the vicinity of the radar location. The biases in both Rayleigh<sub>clear</sub> and Mie<sub>cloudy</sub> are close to zero, whereas the random errors are found to be  $4.87 \text{ m s}^{-1}$  and  $3.77 \text{ m s}^{-1}$ , respectively. It can be seen that overall, the systematic and random errors in Rayleigh<sub>clear</sub> and Mie<sub>cloudy</sub> for 2B10 are very close to 2B11, which shows the mutual consistency of recent Aeolus wind products.

Additionally the accuracy of Rayleigh HLOS wind for cloudy sky conditions (Rayleigh<sub>cloudy</sub>) and Mie for clear conditions (Mie<sub>clear</sub>) in 2B11 is assessed. It is found that bias, SD and SMAD are higher than their clear and cloudy counterparts. Although the bias is close to zero for Rayleigh<sub>cloudy</sub>, the SD and SMAD values are  $6.10 \text{ m s}^{-1}$  and  $5.86 \text{ m s}^{-1}$ ,

**Table 2.** Statistics Comparing Aeolus and Radar's HLOS wind for 2B11. R is the Pearson correlation coefficient and N is the number of data points used for the statistics. Asc and Dsc refer to ascending and descending orbits. Values within brackets indicate statistics for comparison with a temporal difference of  $\pm 1$  hours.

	Rayleigh <sub>clear</sub>						Mic <sub>cloudy</sub>					
	Bias (m s <sup>-1</sup> )	SD (m s <sup>-1</sup> )	SMAD (m s <sup>-1</sup> )	R	N		Bias (m s <sup>-1</sup> )	SD (m s <sup>-1</sup> )	SMAD (m s <sup>-1</sup> )	R	N	
Baseline	-0.15 (0.003)	5.49 (5.40)	4.87 (4.76)	0.93 (0.92)	674 (591)		-0.06 (-0.10)	4.80 (5.05)	3.68 (3.77)	0.94 (0.94)	964 (784)	
2B11 <sub>Asc</sub>	0.06 (0.13)	5.37 (5.37)	4.7 (4.65)	0.92 (0.91)	582 (536)		-0.075 (-0.49)	4.82 (5.02)	3.67 (3.83)	0.93 (0.93)	875 (746)	
2B11 <sub>Dsc</sub>	-1.59 (-1.24)	5.78 (5.51)	5.99 (6.11)	0.93 (0.92)	92 (55)		0.04 (-1.12)	4.60 (5.03)	3.62 (3.06)	0.95 (0.92)	89 (38)	

**Table 3.** Same as Table 2, but for 2B10.

Baseline	Rayleigh <sub>clear</sub>						Mie <sub>cloudy</sub>					
	Bias (m s <sup>-1</sup> )	SD (m s <sup>-1</sup> )	SMAD (m s <sup>-1</sup> )	R	N		Bias (m s <sup>-1</sup> )	SD (m s <sup>-1</sup> )	SMAD (m s <sup>-1</sup> )	R	N	
2B10	-0.018 (0.08)	5.37 (5.22)	5.05 (4.59)	0.95 (0.94)	394 (351)		-0.09 (-0.09)	4.22 (4.63)	3.57 (3.87)	0.96 (0.95)	608 (498)	
2B10 <sub>A5c</sub>	0.29 (0.24)	5.22 (5.17)	4.73 (4.47)	0.93 (0.93)	355 (323)		-0.13 (-0.05)	4.43 (4.69)	3.59 (3.92)	0.95 (0.94)	568 (477)	
2B10 <sub>D5c</sub>	-2.86 (-1.89)	6.01 (5.58)	7.02 (6.71)	0.98 (0.94)	39 (28)		0.53 (-1.05)	4.20 (3.02)	3.40 (2.74)	0.97 (0.98)	40 (21)	

respectively. In case of  $Mie_{clear}$  bias, SD and SMAD are  $-6.50 \text{ m s}^{-1}$ ,  $8.00 \text{ m s}^{-1}$  and  $9.9 \text{ m s}^{-1}$ , respectively. It is to be mentioned that the number of collocated samples obtained for  $Rayleigh_{cloudy}$  and  $Mie_{clear}$  are much lesser after applying a threshold on error estimate and they are 91 and 21, respectively. Therefore, the relatively larger error in  $Mie_{clear}$  as compared to  $Rayleigh_{cloudy}$  may be due to the differences in the number of collocated samples.

### 3.2. Aeolus wind error as a function of altitude, season and wind speed

The HLOS winds from Aeolus and radar for various altitude bins and their difference are shown in Figure 4 for  $Rayleigh_{clear}$ . The mean wind, bias and its significance (standard error) have been shown for altitude bins of 2 km thickness for satisfying the necessary sample size to derive robust statistics. In general, the Aeolus wind profiles match very well with radar and are able to capture the altitude variations in the wind quite well. Though the biases are less than  $1 \text{ m s}^{-1}$  for 1–13 km altitude range, the largest bias (SD) is seen within 15–17 km which is  $-1.13 \text{ m s}^{-1}$  ( $6.74 \text{ m s}^{-1}$ ).

The bias in Aeolus as a function of observed wind speed from the radar is shown in Figure 5(a,b). The mean wind speed from Aeolus shows very good agreement with radar for different wind speed ranges. The bias is found to be less than  $1 \text{ m}$

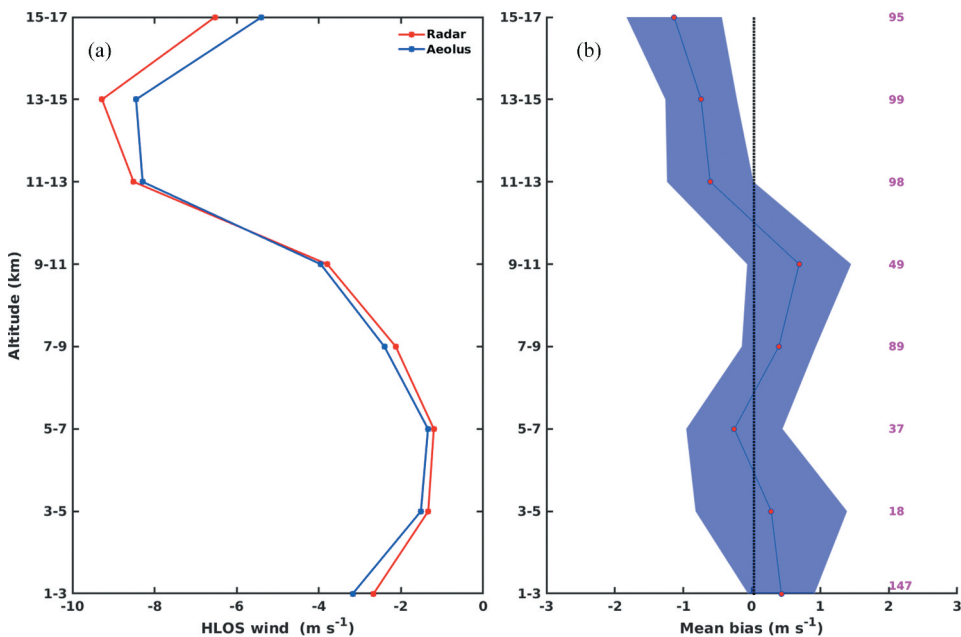


**Figure 4.** (a) Mean HLOS wind from Aeolus (2B11) and radar for various altitude bins of thickness 2 km for  $Rayleigh_{clear}$ . (b) Bias as a function of altitude bins. The shaded region is the standard error,  $\sigma/\sqrt{N}$ , where  $\sigma$  is the standard deviation and  $N$  is the number of data points at each bin. The numbers in magenta represent number of data points used at each altitude bin. Data time period is from July 2019 to September 2021.

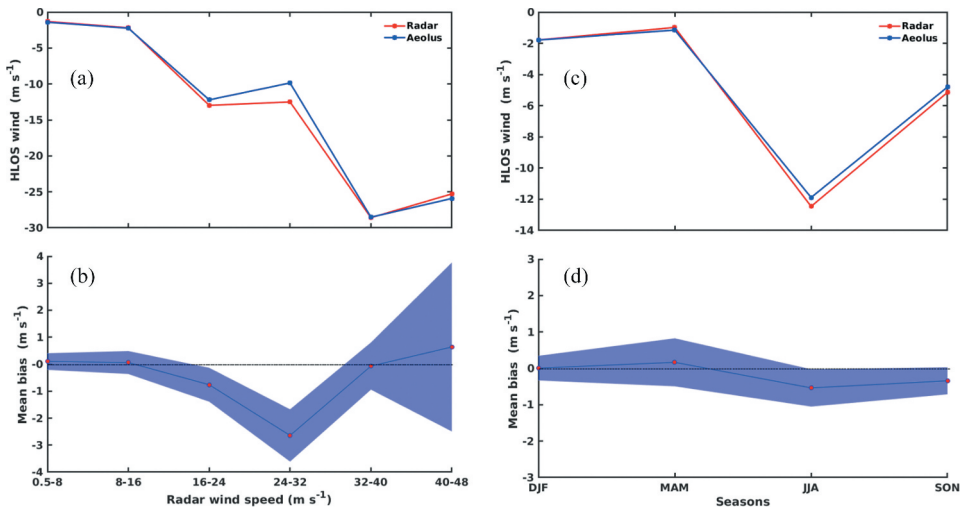


**Figure 5.** (a) Mean HLOS wind from Aeolus (2B11) and radar as a function of observed radar wind speed for  $\text{Rayleigh}_{\text{clear}}$ . (b) Bias as a function of wind speed. (c) Mean HLOS wind from Aeolus and radar as a function of seasons. (d) Bias as a function of seasons. The shaded region is the standard error,  $\sigma/\sqrt{N}$ , where  $\sigma$  is the standard deviation and  $N$  is the number of data points at each bin. Data time period is from July 2019 to September 2021.

$\text{s}^{-1}$  below  $24 \text{ m s}^{-1}$ , but bias seems to be large within  $24\text{--}33 \text{ m s}^{-1}$ . This is due to the presence of collocated pairs which fall in the tail of probability distribution (see Figure 3(c)) in that speed bin. Although the bias is below  $1 \text{ m s}^{-1}$  above  $40 \text{ m s}^{-1}$ , its significance is low due to few number of data points (10) in that bin. The differences in the Aeolus wind with respect to radar for different seasons are shown in Figure 5(c,d). Here the comparison period is divided into four seasons, namely, winter (December, January, February–DJF), spring (March, April, May–MAM), summer (June, July, August–JJA) and autumn (September, October, November–SON). This segregation has been made to improve the robustness of the comparison. The mean Aeolus wind is in good agreement with radar for all seasons, and the bias values are below  $1 \text{ m s}^{-1}$  and are not observed to have any seasonal dependence.

The bias in  $\text{Mie}_{\text{cloudy}}$  as a function of altitude is shown in Figure 6. As observed for  $\text{Rayleigh}_{\text{clear}}$ ,  $\text{Mie}_{\text{cloudy}}$  wind also has an altitude dependent bias. The bias values range from  $-1.75$  to  $2.25 \text{ m s}^{-1}$ , where the smallest value of  $0.0060 \text{ m s}^{-1}$  is seen within  $11\text{--}13 \text{ km}$  and the largest value of  $2.25 \text{ m s}^{-1}$  is observed between  $13\text{--}17 \text{ km}$ . The biases between Aeolus and radar are minimal up to a speed range of  $0.5\text{--}40 \text{ m s}^{-1}$  (Figure 7(a,b)). The values are below  $1 \text{ m s}^{-1}$  in the said range with standard deviations below  $\pm 5 \text{ m s}^{-1}$ . The bias and standard deviations are larger at higher wind speeds (above  $40 \text{ m s}^{-1}$ ). The observed bias (SD) is  $3.94 \text{ m s}^{-1}$  ( $9.71 \text{ m s}^{-1}$ ), however the number of data points in that particular wind speed range is much lower (23) when compared to other bins. This is true for  $\text{Rayleigh}_{\text{clear}}$  as well, therefore, the confidence in this error estimate is low. The differences in HLOS wind between radar and Aeolus for different seasons are shown in Figure 7(c,d).

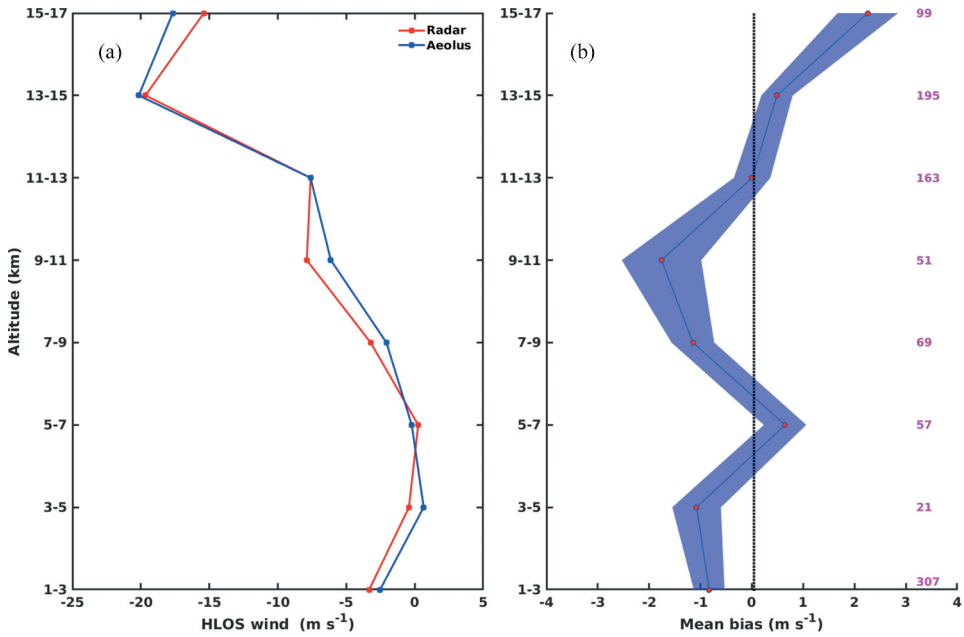


Figure 6. Same as Figure 4 but for Mie<sub>cloudy</sub>.

The biases are close to zero for all seasons except during spring where it is above 1 m s<sup>-1</sup>. This could be due to lesser number of data points used in spring (128 data) for statistics as compared to other seasons (more than 240). The standard deviations are slightly higher than 4 m s<sup>-1</sup> for all seasons.

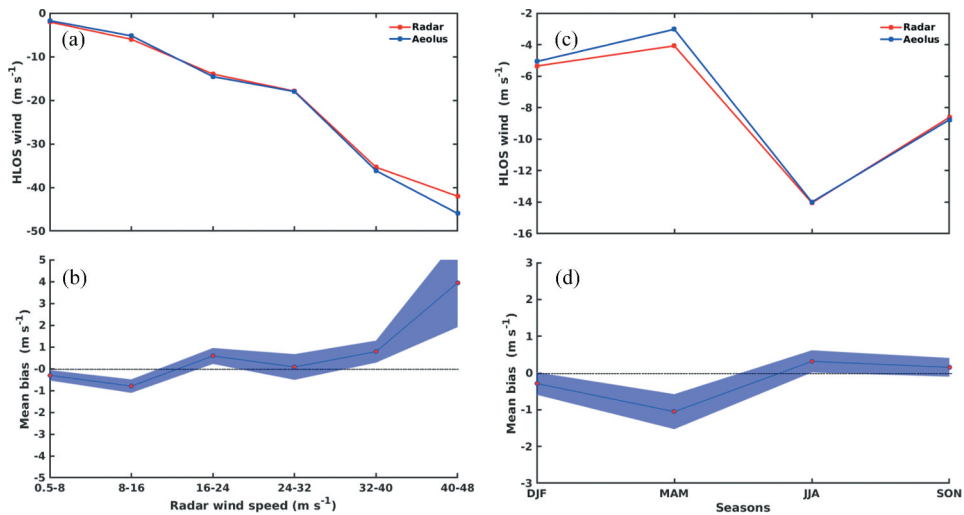


Figure 7. Same as Figure 5 but for Mie<sub>cloudy</sub>.

## 4. Summary and discussion

This paper presents a comprehensive validation of Aeolus horizontal line-of-sight wind over Cochin (10.04° N, 76.9°E), India using the state-of-the-art 205 MHz wind profiler radar. The quality of Aeolus level 2 wind baseline products 2B10 and 2B11 have been assessed for the period July 2019 to September 2021. The errors in the Aeolus wind profiles with respect to radar between 1 and 18 km altitude are evaluated. The Aeolus wind profiles have been validated by comparing them with collocated radar wind measurements.

The Aeolus wind shows good capability in measuring the atmospheric wind variability for the altitude range of 1–18 km. The mean bias between 2B11 (2B10) Aeolus and radar HLOS wind is found to be  $-0.15 \text{ m s}^{-1}$  ( $-0.018 \text{ m s}^{-1}$ ) for Rayleigh<sub>clear</sub> and  $-0.006 \text{ m s}^{-1}$  ( $-0.009 \text{ m s}^{-1}$ ) in Mie<sub>cloudy</sub>. The random error in Rayleigh<sub>clear</sub> for 2B11 (2B10) is observed to be  $4.87 \text{ m s}^{-1}$  ( $5.05 \text{ m s}^{-1}$ ), whereas the corresponding value for Mie<sub>cloudy</sub> is  $3.68 \text{ m s}^{-1}$  ( $3.57 \text{ m s}^{-1}$ ). The Aeolus wind profiles match well with the observed wind speeds from the radar in all the seasons. A detailed analysis of Aeolus wind in different altitudes shows that the wind is more biased between 15–17 km as compared to lower layers for both Rayleigh and Mie. Although Aeolus wind shows a large bias in high wind speed ranges, the significance of the error estimate is low due to limited number of collocated datasets. The systematic and random errors in Aeolus wind between ascending and descending orbits do not vary much for Rayleigh and Mie.

Studies undertaken in the past have shown different values for random and systematic errors in Aeolus wind. Martin et al. (2021) have shown that the bias (random error) is in the range of  $1.8\text{--}2.8 \text{ m s}^{-1}$  ( $4.1\text{--}4.4 \text{ m s}^{-1}$ ) for Rayleigh clear and  $1.3\text{--}1.9 \text{ m s}^{-1}$  ( $1.9\text{--}3.0 \text{ m s}^{-1}$ ) for Mie cloudy. The random errors for Aeolus wind reported in our study is in agreement with Martin et al. (2021), but systematic errors have differences. Baars et al. (2020) show that systematic and random errors in Aeolus wind are in the order of  $1.5 \text{ m s}^{-1}$  and  $4.84 \text{ m s}^{-1}$ , respectively for Rayleigh whereas the corresponding values are  $1 \text{ m s}^{-1}$  and  $1.5 \text{ m s}^{-1}$  for Mie. Although the random error in Rayleigh shown in Baars et al. (2020) agree with our study, it is not the case for Mie wind. This could be because they have used baseline 2B02, and it is shown in Iwai et al. (2021) that errors are more in 2B02 as compared to 2B10. Random errors in Rayleigh and Mie shown in Iwai et al. (2021) are  $5.1$  and  $4.8 \text{ m s}^{-1}$ , respectively, for 2B10 with systematic errors less than  $1 \text{ m s}^{-1}$ . The random error in Rayleigh wind in this study is close to our results while it differs by more than  $1 \text{ m s}^{-1}$  in Mie cloudy wind. A recent study by Rani et al. (2022) shows that over the tropics, random error in Rayleigh clear (Mie cloudy) is  $8 \text{ m s}^{-1}$  ( $5 \text{ m s}^{-1}$ ) while the systematic errors are close to zero in both cases. They have drawn their results from a comparatively shorter duration (June–August 2020) of data.

The overall errors in Aeolus wind shown in this study are consistent with the general consensus that the random errors in Rayleigh clear (Mie cloudy) are in the range of  $5\text{--}6 \text{ m s}^{-1}$  ( $3.5\text{--}4 \text{ m s}^{-1}$ ) with systematic errors close to zero (Straume-Lindner et al. 2021). This

study shows that Aeolus wind is of good quality and also highlights the use of exceptional data from 205 MHz wind profiler for the validation of satellite winds.

## Acknowledgement

The financial support provided by the Ministry of Earth Sciences (MoES), Government of India for the sustenance of the ST Radar Facility is greatly acknowledged. Roshny Antony would like to thank the Department of science and technology for their research support through WOS-A. Many thanks to Prof. Sheila Kirkwood for her inputs on Aeolus data reading. We thank the reviewers for their useful comments that have resulted in improving the content and quality of the paper.

## Disclosure statement

No potential conflict of interest was reported by the author(s).

## Funding

The author(s) reported there is no funding associated with the work featured in this article.

## ORCID

S Abhilash  <http://orcid.org/0000-0002-3834-8737>

## References

- Baars, H., A. Herzog, B. Heese, K. Ohneiser, K. Hanbuch, J. Hofer, Z. Yin, R. Engelmann, and U. Wandinger. 2020. "Validation of Aeolus Wind Products Above the Atlantic Ocean." *Atmospheric Measurement Techniques* 13 (11): 6007–6024. doi:10.5194/amt-13-6007-2020.
- Belova, E., S. Kirkwood, P. Voelger, S. Chatterjee, K. Satheesan, S. Hagelin, M. Lindskog, and H. Körnich. 2021. "Validation of Aeolus Winds Using Ground-Based Radars in Antarctica and in Northern Sweden." *Atmospheric Measurement Techniques* 14 (8): 5415–5428. <https://amt.copernicus.org/articles/14/5415/2021/>
- ECMWF:Rennie, M. T., P. Andersson, A. Dabas, J. M. de Kloe, and A. Stoffelen. 2020. "Aeolus Level-2b480algorithm Theoretical Basis Document (Mathematical Description of the Aeolus Level-2B Processor)." *Technical Report*. AE-TN-ECMWF-L2BP.0023,V.3.21.
- Iwai, H., M. Aoki, M. Oshiro, and S. Ishii. 2021. "Validation of Aeolus Level 2B Wind Products Using Wind Profilers, Ground-Based Doppler Wind Lidars, and Radiosondes in Japan." *Atmospheric Measurement Techniques* 14 (11): 7255–7275. <https://amt.copernicus.org/articles/14/7255/2021/>
- Khaykin, S. M., A. Hauchecorne, R. Wing, P. Keckhut, S. Godin-Beekmann, J. Porteneuve, J.-F. Mariscal, and J. Schmitt. 2020. "Doppler Lidar at Observatoire de Haute-Provence for Wind Profiling Up to 75 Km Altitude: Performance Evaluation and Observations." *Atmospheric Measurement Techniques* 13 (3): 1501–1516. <https://amt.copernicus.org/articles/13/1501/2020/>
- Kottayil, A., K. Mohanakumar, T. Samson, M. M. Rejoy Rebello, K. S. Rakesh Varadarajan, P. Mohanan, and K. Vasudevan. 2016. "Validation of 205 Mhz Wind Profiler Radar Located at Cochin, India, Using Radiosonde Wind Measurements." *Radio Science* 51 (3): 106–117. doi:10.1002/2015RS005836.

- Kottayil, A., K. Satheesan, K. Mohankumar, S. Chandran, and T. Samson. 2018. "An Investigation into the Characteristics of Inertia Gravity Waves in the Upper Troposphere/lower Stratosphere Using a 205 Mhz Wind Profiling Radar." *Remote Sensing Letters* 9 (3): 284–293. doi:10.1080/2150704X.2017.1418991.
- Kottayil, A., K. S. Prince Xavier, K. Mohanakumar, and V. Rakesh, V. Rakesh. 2020. "Vertical Structure and Evolution of Monsoon Circulation as Observed by 205-Mhz Wind Profiler Radar." *Meteorology and Atmospheric Physics* 132 (4): 531–545. doi:10.1007/s00703-019-00695-4.
- Legras, B. and S. Bucci. 2020. "Confinement of Air in the Asian Monsoon Anticyclone and Pathways of Convective Air to the Stratosphere During Summer Season." *Atmospheric Chemistry and Physics* 20 (18): 11045–11064. doi:10.5194/acp-20-11045-2020.
- Lux, O., C. Lemmerz, F. Weiler, U. Marksteiner, B. Witschas, S. Rahm, A. Geiß, and O. Reitebuch. 2020. "Intercomparison of Wind Observations from the European Space Agency's Aeolus Satellite Mission and the ALADIN Airborne Demonstrator." *Atmospheric Measurement Techniques* 13 (4): 2075–2097. <https://amt.copernicus.org/articles/13/2075/2020/>
- Martin, A., M. Weissmann, O. Reitebuch, M. Rennie, A. Geiß, and A. Cress. 2021. "Validation of Aeolus Winds Using Radiosonde Observations and Numerical Weather Prediction Model Equivalents." *Atmospheric Measurement Techniques* 14 (3): 2167–2183. <https://amt.copernicus.org/articles/14/2167/2021/>
- Mohanakumar, K., V. A. Ajil Kottayil, T. Samson, K. S. Linto Thomas, and R. Rebello, K. Satheesan, R. Rebello, et al. 2017. "Technical Details of a Novel Wind Profiler Radar at 205 Mhz." *Journal of Atmospheric and Oceanic Technology* 34 (12): 2659–2671. doi:10.1175/JTECH-D-17-0051.1.
- Nieman, S. J., J. Schmetz, and W. Paul Menzel. 1993. "A Comparison of Several Techniques to Assign Heights to Cloud Tracers." *Journal of Applied Meteorology* 32 (9): 1559–1568. doi:10.1175/1520-0450(1993)032<1559:ACOSTT>2.0.CO;2.
- Nithya, K., A. Kottayil, and K. Mohanakumar. 2019. "Determining the Tropopause Height from 205 Mhz Stratosphere Troposphere Wind Profiler Radar and Study the Factors Affecting Its Variability During Monsoon." *Journal of Atmospheric and Solar-Terrestrial Physics* 182: 79–84. doi:10.1016/j.jastp.2018.10.018.
- Rani, S. I., B. Prakash Jangid, M. T. B. Sumit Kumar, P. Sharma, J. P. George, G. George, and M. Das Gupta. 2022. "Assessing the Quality of Novel Aeolus Winds for NWP Applications at NCMRWF." *Quarterly Journal of the Royal Meteorological Society* 148 (744): 1344–1367. doi:10.1002/qj.4264.
- Reitebuch, O. 2012. *The Spaceborne Wind Lidar Mission ADM-Aeolus*, 815.
- Rennie, M. and L. Isaksen. 2020. "The NWP Impact of Aeolus Level-2B Winds at ECMWF." 864. <https://www.ecmwf.int/node/19538>.
- Rennie, M. P., L. Isaksen, F. Weiler, J. de Kloe, T. Kanitz, and O. Reitebuch. 2021. "The Impact of Aeolus Wind Retrievals on ECMWF Global Weather Forecasts." *Quarterly Journal of the Royal Meteorological Society* 147 (740): 3555–3586. <https://rmets.onlinelibrary.wiley.com/doi/abs/10.1002/qj.4142>
- Satheesan, K. and B. V. Krishna Murthy. 2002. "Turbulence Parameters in the Tropical Troposphere and Lower Stratosphere." *Journal of Geophysical Research (Atmospheres)* 107 (D1): 4002. doi:10.1029/2000JD000146.
- Schmetz, J., K. Holmlund, J. Hoffman, B. Strauss, B. Mason, V. Gaertner, A. Koch, and L. van de Berg. 1993. "Operational Cloud-Motion Winds from Meteosat Infrared Images." *Journal of Applied Meteorology* 32 (7): 1206–1225. doi:10.1175/1520-0450(1993)032<1206:OCMWF>2.0.CO;2.
- Stoffelen, A., J. Pailleux, J. M. V. Erland Källén, L. Isaksen, P. Flamant, and W. Wergen, W. Wergen, et al. 2005. "The Atmospheric Dynamics Mission for Global Wind Field Measurement." *Bulletin of the American Meteorological Society* 86 (1): 73–87. doi:10.1175/BAMS-86-1-73.
- Straume-Lindner, A. G., T. Parrinello, J. Von Bismarck, S. Bley, D. Wernham, T. Kanitz, E. Alvarez, et al. 2021. "ESA'S Wind Mission Aeolus - Overview, Status and Outlook." In *2021 IEEE International Geoscience and Remote Sensing Symposium IGARSS Brussels, Belgium*, 755–758.

- Sujithlal, S., K. Satheesan, K. Ajil, and K. Mohanakumar. 2022. "Observation of Stratosphere–troposphere Exchange During a Pre-Monsoon Thunderstorm Activity Over Kochi, India." *Meteorology and Atmospheric Physics* 134 (3). doi:[10.1007/s00703-022-00893-7](https://doi.org/10.1007/s00703-022-00893-7).
- Witschas, B., C. Lemmerz, and O. Reitebuch. 2012. "Horizontal Lidar Measurements for the Proof of Spontaneous Rayleigh-Brillouin Scattering in the Atmosphere." *Applied Optics* 51 (25): 6207. doi:[10.1364/AO.51.006207](https://doi.org/10.1364/AO.51.006207).
- Witschas, B., C. Lemmerz, A. Geiß, O. Lux, U. Marksteiner, S. Rahm, O. Reitebuch, and F. Weiler. 2020. "First Validation of Aeolus Wind Observations by Airborne Doppler Wind Lidar Measurements." *Atmospheric Measurement Techniques* 13 (5): 2381–2396. doi:[10.5194/amt-13-2381-2020](https://doi.org/10.5194/amt-13-2381-2020).